Microgrid Communications Using the Open-Source Open Field Message Bus (OpenFMB) Framework Applied to a 480V, 100kW Laboratory Microgrid

Maximiliano Ferrari
Oak Ridge National Laboratory (ORNL)
Grid Components and Controls Group
Oak Ridge, US
ferrarimagmf@ornl.gov

Aditya Sundararajan
Oak Ridge National Laboratory (ORNL)
Grid Components and Controls Group
Oak Ridge, US
sundararajaa@ornl.gov

Neil Shepard
Oak Ridge National Laboratory (ORNL)
Grid Components and Controls Group
Oak Ridge, US
shepardne@ornl.gov

John Smith
Oak Ridge National Laboratory (ORNL)
Grid Components and Controls Group
Oak Ridge, US
smithjrjjjr@ornl.gov

Ben Ollis
Oak Ridge National Laboratory (ORNL)
Grid Components and Controls Group
Oak Ridge, US
ollistb@ornl.gov

***Abstract*—Microgrids require an extensive communication infrastructure to allow interoperability between the microgrid controller and assets. However, the lack of standardization of data structures combined with the variety of communication protocols poses several challenges to the implementation of a communication network. This paper presents an application of the open-source Open Field Message Bus (OpenFMB) framework to simplify the communication layer in microgrids. This work leverages the OpenFMB protocol translation and data model extensions to reduce the complexity in the microgrid communications. Conducted in a laboratory microgrid, the case study demonstrates how the OpenFMB provides predefined data models and simplifies the communication layer by providing information exchange between multiple legacy communication protocols.**

Keywords—Microgrid, Communications, DNP3, Modbus, OpenFMB

I. INTRODUCTION

Microgrids have been identified as a critical component for improving power reliability, increasing energy system efficiency, enabling higher integration of renewable energy sources, and providing energy independence from the grid to end-users. Microgrids have been defined in multiple ways in the literature [1-3]. In essence, a microgrid is a section of the electric grid that retains its connection to the centralized grid most of the time but can "island" itself and operate for hours or even days at a time independently from the centralized grid.

The U.S. Department of Energy describes a microgrid as "a group of interconnected loads and distributed energy resources within clearly defined electrical boundaries that acts as a single controllable entity with respect to the grid. A microgrid can connect and disconnect from the grid to enable it to operate in both grid-connected and island-mode.'' [2].

The implementation of microgrid architectures involves the participation of many distributed energy resources (DERs), protection devices, controllable loads, and metering, which are required to operate in coordination with the microgrid controller to meet local objectives. This level of interoperability requires an extensive communication network to allow the communication between the microgrid controller and the microgrid assets. Unfortunately, the lack of standardization of the data structure, combined with the variety of communication protocols utilized by the microgrid assets, make the communication network in microgrids very challenging [4]. From an engineering perspective, the communication layer must be tailor-fitted for every new microgrid project, which impacts the engineering costs of the project.

This paper presents an application of the open-source Open Field Message Bus (OpenFMB) framework to reduce the complexity associated with microgrid communications. In this work, the OpenFMB framework was used to translate legacy protocols (such as Modbus and DNP3) to a common publish/subscribe messaging protocol based on NATS. This paper leverages the OpenFMB data models, which encompasses the data exchanged between the microgrid controller and the microgrid assets. The case study carried out on a 480V, 100kW microgrid testbed exemplifies how OpenFMB is effective in simplifying the communication layer by providing bidirectional exchange of information between microgrid controller and legacy protocols of the microgrid assets.

ACKNOWLEDGEMENTS Research sponsored by the Laboratory Directed Research and Development Program of Oak Ridge National Laboratory, P.O. Box 2008, Oak Ridge, Tennessee 37831-6285; managed by UT Battelle, LLC, for the U.S. Department of Energy. This manuscript has been authored by UT-Battelle, LLC, under contract DE-AC05- 00OR22725 for the U.S. Department of Energy. The United States Government retains and the publisher, by accepting the article for publication, acknowledges that the United States Government retains non-exclusive, paid-up, irrevocable, worldwide license to publish or reproduce the published form of this manuscript, or allow others to do so, for United States Government purposes. This material is based upon work supported by the U.S. Department of Energy's Office of Energy Efficiency and Renewable Energy (EERE) under the Solar Energy Technologies Office Award Number DE-EE0002243-2144

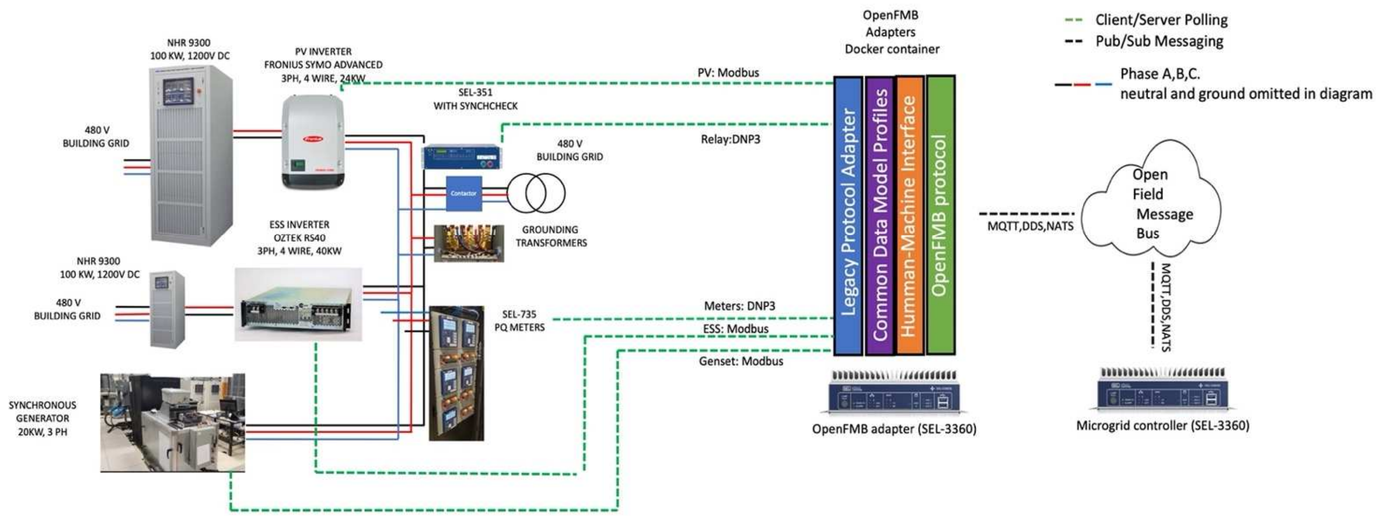

Fig. 2. OpenFMB reference architecture applied to the 480V, 100 kW laboratory microgrid testbed.

II. OpenFMB Architecture

The basic OpenFMB operational architecture, modeled after [5], is shown in Fig. 1. It consists of three major components: application, adapter layers and an interface layer [5]. I) The *applications* are located within an OpenFMB node and hosts the OpenFMB Adapters or OpenFMB applications. II) *The protocol adapters* are located within an OpenFMB node and interface the field message bus with end devices. They provide unidirectional or bi-directional exchange of in-formation between data models and legacy protocols and conventional formats, such as DNP3, Modbus, IEC 61850 ACSI, C12, CoAP, XMPP, or others. III) *The interface layer* provides data profiles, interfaces to appropriate publish-subscribe protocols, security, and other services. Data models describe the message payloads exchanged among various OpenFMB adapters and OpenFMB applications.

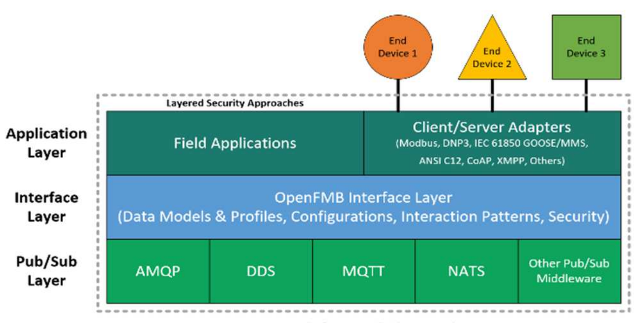

Fig. 1. OpenFMB operational logical architecture [8].

III. Data Modelling and Interoperability

The information exchange in the OpenFMB framework is based on predefined data models. The OpenFMB data model is built based on both IEC CIM and 61850 standards. The IEC CIM provides a mature messaging data structure for OpenFMB models. The IEC 61850 offers detailed device attributes. The objective of the IEC 61850 is to enable vendor independent application interoperability [5-7]. The data structure represents a hierarchical structure with multiple data objects grouped under a logical node representing a physical device. Each device in the microgrid has its own data model. For instance, the OpenFMB adapter for the energy storage unit has a reading and a control data model, also called data profile. The reading profile maps the analog registers for the Energy Storage System (ESS), such as currents, voltage, frequency, reactive power, and active power. The control profile maps the registers required for black start, shutdown, and the setpoints for voltage, frequency, and active and reactive power. After this data profile is created, it becomes the the standard profiles for other ESS units in the microgrid. The data profiles facilitate the addition of additional ESS units, which follow the same data structure and only require remapping to reflect the registers in the new unit.The operational model for the ESS control profile is presented as an example in Fig. 3(a). Fig. 3(b) shows the data profiles for the Modbus devices, which are the ESS and PV inverter. The DNP3 devices have a separate profile and are not shown in the figure. A full list of data profiles supported by OpenFMB are available in [9].

IV. OPENFMB FRAMEWORK APPLIED TO HARDWARE MICROGRID TESTBED

Fig. 2. shows that OpenFMB framework applied to the 100kW, 480V microgrid testbed. The testbed is a state-of-the-art laboratory network microgrid located at Oak Ridge National Laboratory, Oak-ridge, Tennessee. The three-phase, 4-wire microgrid runs at 480Vrms and consists of a 40kW Oztek energy storage inverter (ES), 24kW Fronius Symo Advanced PV inverter, and a 20kW synchronous machine. Each PV inverter and ESS inverter are coupled in the dc side to 100kW NHR 9300 DC supplies. The NHR 9340 4-quadrant regenerative emulator is used as active controllable load with a capacity of 100 kW. The test microgrid can operate in island or grid tied mode. In island mode the voltage and frequency source can be either the ESS or the synchronous machine. In grid-tied mode, the 480V bulk grid provides the voltage and frequency reference and the ESS and genset transition to active and reactive power control mode (PQ mode). The microgrid testbed includes SEL protection devices which are programmed with synchcheck capabilities. Power quality meters are installed in the microgrid to provide the microgrid controller with the required measurements to perform the optimization tasks.

As mentioned, the OpenFMB framework was implemented in the microgrid using OpenFMB adapters. The adapter is a portable version of OpenFMB and acts as a translator for legacy protocols, allows bidirectional communication with the microgrid controller using a predefined data structure for each of the microgrid assets. As seen in Fig. 2., the different protocols are utilized for the DERs and protective devices in the laboratory microgrid. The protocol for protection relay SEL 351 is DNP-3. Both the Fronius PV inverter and the Oztek Energy Storage Systems (ESS) use Modbus as their communication protocol. The Power quality meters are also based on DNP3. In this work, a containerized version of the OpenFMB adapter is implemented on Linux machine installed in a hardened industrial computer SEL-3360. This open-source version runs on a Docker container, and it is available to the public in [4].

V. EXPERIMENTAL RESULS

This section presents the experimental results utilizing the microgrid testbed with OpenFMB as communication framework. The use-case narrative for the tests consists of preparing the microgrid for an intentional island operation triggered by a planned outage caused by a severe storm. For the experiments, the microgrid assets were controlled using the Human-Machine Interface HMI interface provided by OES [4]. Because the focus of this paper is the communication network, the evaluation of the microgrid controller is out of the scope of this paper and will be addressed in future publications. For practical reasons, the test was programmed in the laboratory testbed to last minutes, instead of the hours that this event would take in a real demonstration in the field. All the communications required for the presented use case were stablished through the OpenFMB adapter.

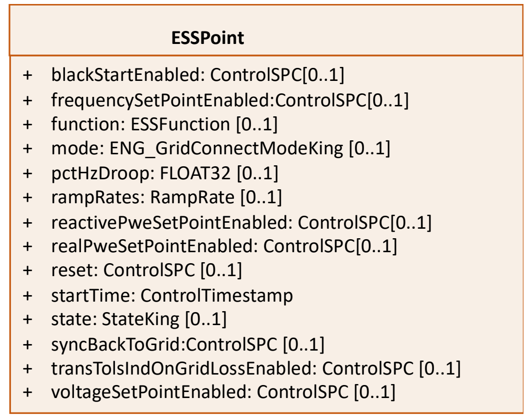

(a)

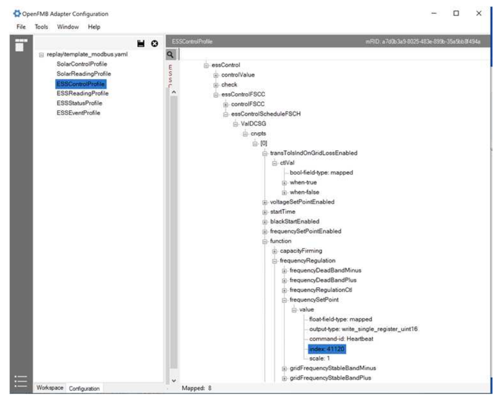

(b)

Fig.3. (a) OpenFMB operational models for ESS control based on IEC 6185 [9]. (b) OpenFMB data models for Modbus devices. Highlighted the control for the Oztek ESS frequency setpoint.

As shown in Fig. 4(A), preventive strategies command the energy storage to charge at a -7kW rate while the grid is healthy with the objective of achieving the highest State of Charge (SOC) possible. In the beginning of the test, both the PV inverter and the grid charge the batteries. Fig. 6 shows a screenshot of the OpenFMB HMI interface that shows the voltages and currents magnitudes during this operating region. At t=70s, the PV output drops from 10kW to 2kW, and power to charge the energy storage and the local loads solely relies on the bulk grid. At t=90s the microgrid is intentionally islanded by sending an open command through the OpenFMB adapter to the Point of Common Coupling (PCC) breaker controlled by a SEL 351. As shown, the transition to island is seamless, and the voltage remains constant with no power loss during the transition to island. During this transition, the energy storage changes from active power and reactive control (PQ) to droop control VF. This transition is possible using a physical digital that between the SEL 351 and the Oztek ESS inverter. Right after the transition, the energy storage discharges to support the local critical loads. Fig. 7 shows a screenshot of the OpenFMB HMI interface that shows the voltages and currents magnitudes during this operating condition, as seen in this figure, the PCC switch is open and the ESS supports the load in the microgrid.

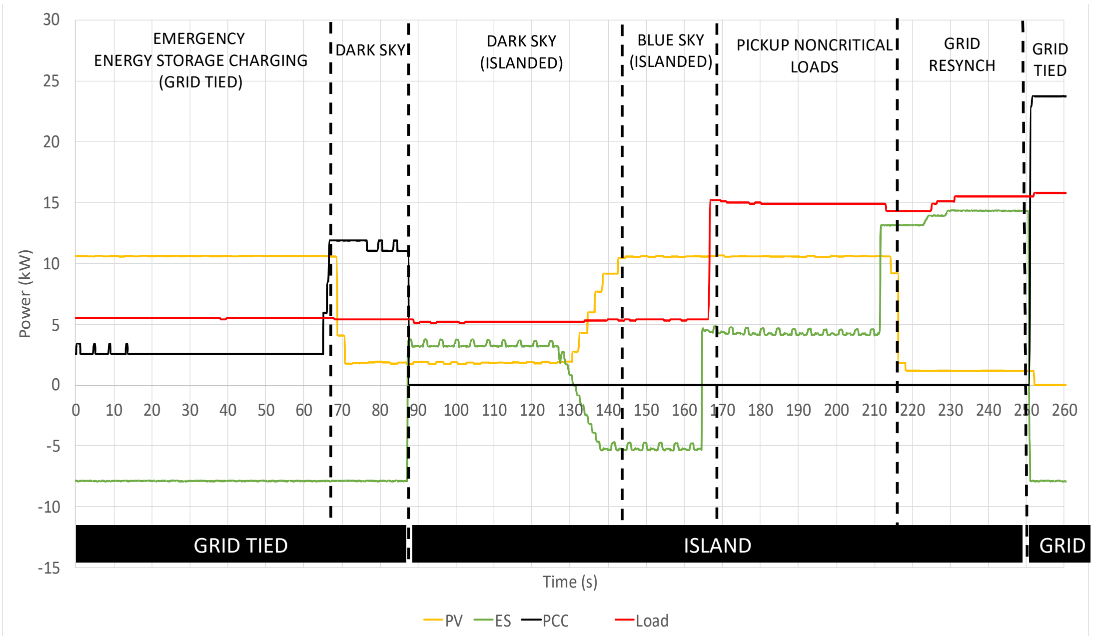

(A)

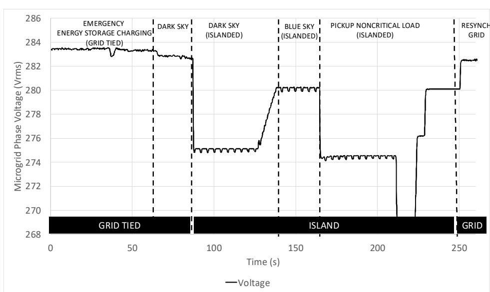

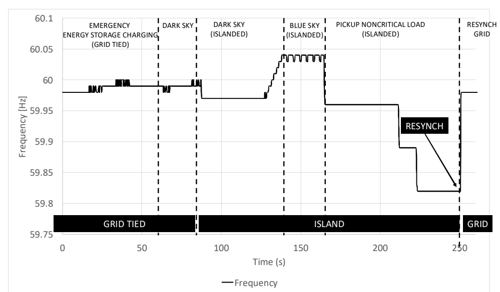

(B) (C)

Fig. 4. (A) Power flow experimental results using the laboratory testbed, which consist of an energy storage inverter rated at 40kW, 24kW of PV generation and a 50kW load. (B) Voltage at the PCC during the test. (C) Frequency profile at the PCC.

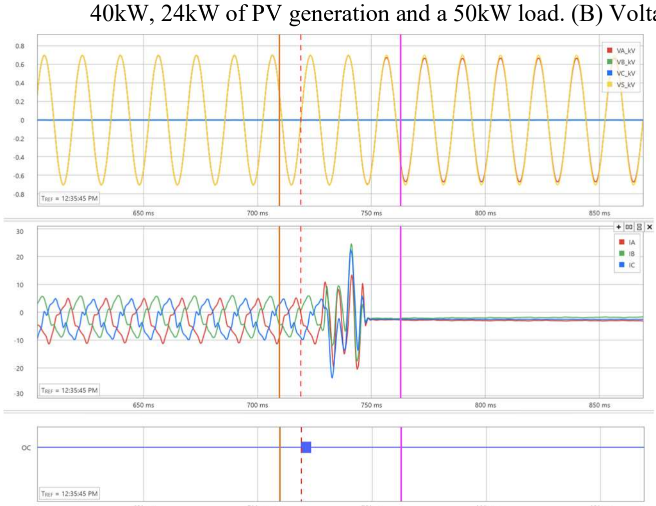

Fig. 5. Grid to island transition. SEL 351 capture, 32 samples per seconds, raw data.

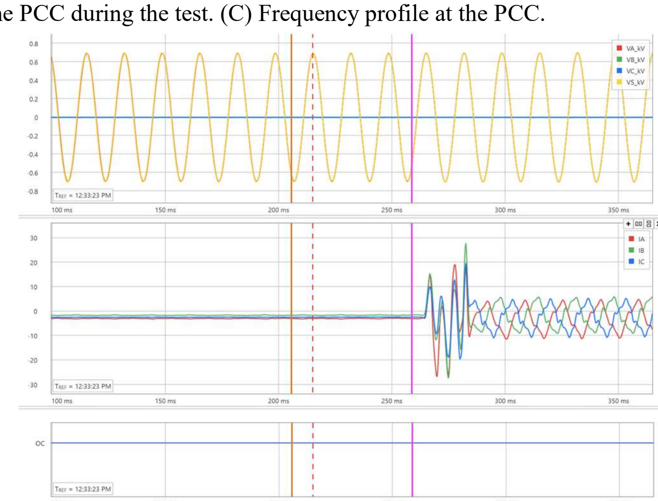

Fig. 6. Island to grid transition. SEL 351 capture, 32 samples per seconds, raw data/

The sky clears at t=130s and the PV output increases back to 10kW. The energy excess in the microgrid is used to charge the energy storage. At t=170s, the PV generation is more than needed, and the microgrid controller commands to connect additional 10kW of non-critical loads. Finally, the grid becomes available at t=215s and the microgrid starts the grid-synchronization sequence. It is commanded to the ESS to change its frequency to increase the likelihood of overlapping the voltages with the grid, which voltages have a frequency of 60Hz. The PV inverter is curtailed to reduce power fluctuations during the transition and a close command is sent to the SEL-351, which controls the point of common coupling (PCC) switch. The synch-check of the SEL 351 waits until the phase, voltage and frequency are withing the desired minimum deviation, which were programmed very stringent to reduce inrush during island to grid transitions. As seen in the figure, after regaining connection to the grid, ESS restarts charging the battery at a rate of -7kW. Fig. 4B-C show the voltage and frequency waveform for the same experiment. See that he voltage and frequency aren't stiff because the Oztek ESS inverter is operating in droop mode. Notice that during islanded operation, the voltage magnitude varies depending on the amount of load and generation. In this figure is also visible low frequency oscillations in the voltage which are caused by the Maximum Power Point Tracking (MPPT) algorithm of the PV Fronius Inverter. During the islanded the voltage always remained withing 5% of deviation. Please notice that the voltage in the figure is phase voltage, not line to line voltage, and its nominal value is approximately 277V.

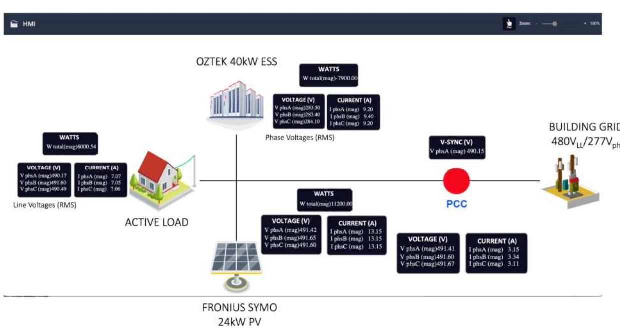

Fig. 7. OpenFMB HMI reflecting the voltages, current and power during the Emergency Energy Storage Charging operation. Grid tied operation.

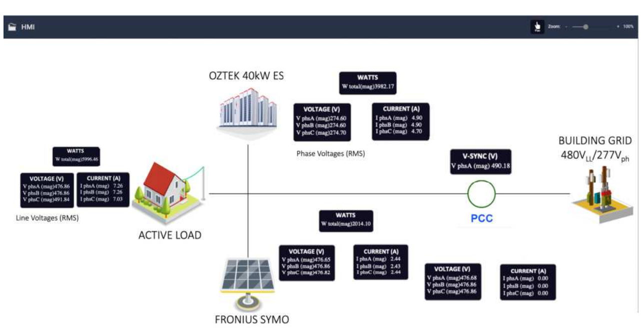

Fig. 8. OpenFMB HMI reflecting the voltages, current and power during Dark Sky operation. Islanded operation.

Fig. 5, and Fig. 6., present the waveforms from the PCC switch that shows the transitions from grid to island and island to grid tied, respectively. These figures show a distorted three-phase currents and the inrush between the modes of operation. The distortion in the current is due to the low magnitude of the current compared with its rated capacity (40kW), at higher power the Total Harmonic Distortion (THD) of the currents improves significatively. The inrush is caused because the because the PCC switch has a mechanical time delay and the energy storage transition from droop control, active during islanding operation, to PQ (Active and Reactive control), which is enabled for grid-tied operation. This inrush did not contain enough energy to trigger any protection in the microgrid or to cause any damage in the microgrid devices.

VI. CONCLUSIONS

This paper presented an application of the open-source Open Field Message Bus (OpenFMB) framework to allow communication the microgrid assets and the microgrid controller. The OpenFMB framework was effective in simplifying the communication layer for the microgrids and provided bidirectional exchange of information between microgrid controller and legacy protocols of the microgrid assets such as DNP3, Modbus. This paper leveraged the OpenFMB data models, which encompasses the data exchanged between the microgrid controller and the microgrid assets. The test was carried out in a state-of-the-art laboratory microgrid located at Oak Ridge National Laboratory, Oak-ridge, Tennessee. The use- case narrative for the tests consists of preparing the microgrid for an intentional island operation triggered by a planned outage caused by a severe storm. All the communication was performed by OpenFMB adapters, and it was shown additional features seamless transitions from both grid to island and island to grid. The future work includes incorporating the microgrid controller and synchronous generation with the microgrid controller, including a technical discussion to enable native to communicate between the OpenFMB adapter and the microgrid controller.

REFERENCES

[1] R. Rossello, A.G. Cuomo, Build Back Better: Reimagining and Strengthening the Power Grid of Puerto Rico and PSEG Long Island, an Agent for and on Behalf of the Long Island Lighting Company D, 2017.

[2] Dan T. Ton, Merrill A. Smith,The U.S. Department of Energy's Microgrid Initiative,The Electricity Journal,Volume 25, Issue 8,2012,Pages 84-94,ISSN 1040-6190,https://doi.org/10.1016/j.tej.2012.09.013.

[3] G. Venkataramanan, C. Marnay, A larger role for microgrids: are microgrids a viable paradigm for electricity supply expansion? IEEE Power Energy Mag. (2008).

[4]https://openfmb.openenergysolutions.com/docs/openfmb/reference

[5] M. Cintuglu, A. Kondabathini and D. Ishchenko, "Real-Time Implementation of Secure Distributed State Estimation for Networked Microgrids," *2020 IEEE 6th World Forum on Internet of Things (WF-IoT)*, 2020, pp. 1-6, doi: 10.1109/WF-IoT48130.2020.9221310.

[6] IEC 61850-7-3: Communication Networks and Systems for Power Utili- ty Automation – Basic Communication Structure – Common Data Clas- ses, Edition 2.0, 2010.
[7] IEC 61850-7-4: Communication
[8] Open Filed Message Bus (OpenFMB), NAESB Standard, March 31, 2016.
[9] https://openfmb.gitlab.io/pim/ops/v2.0.0/index.htm
[10] K. P. Schneider *et al*., "A Distributed Power System Control Architecture for Improved Distribution System Resiliency," in *IEEE Access*, vol. 7, pp. 9957-9970, 2019, doi: 10.1109/ACCESS.2019.2891368.